Available online at www.sciencedirect.com
SCIENCE DIRECT®
Biochemical and Biophysical Research Communications 328 (2005) 292–305
BBRC
www.elsevier.com/locate/ybbrc

An unusual soluble β-turn-rich conformation of prion is involved in fibril formation and toxic to neuronal cells☆

Jurate Kazlauskaite[a], Anna Young[a], Catherine E. Gardner[b], Julie V. Macpherson[b], Catherine Vénien-Bryan[c], Teresa J.T. Pinheiro[a,*]

[a] Department of Biological Sciences, University of Warwick, Gibbet Hill Road, Coventry CV4 7AL, UK
[b] Department of Chemistry, University of Warwick, Coventry CV4 7AL, UK
[c] Laboratory of Molecular Biophysics, University of Oxford, Oxford OX1 3QU, UK

Received 7 December 2004
Available online 7 January 2005

Abstract

A key molecular event in prion diseases is the conversion of the prion protein (PrP) from its normal cellular form (PrP^C) to the disease-specific form (PrP^{Sc}). The transition from PrP^C to PrP^{Sc} involves a major conformational change, resulting in amorphous protein aggregates and fibrillar amyloid deposits with increased β-sheet structure. Using recombinant PrP refolded into a β-sheet-rich form (β-PrP) we have studied the fibrillization of β-PrP both in solution and in association with raft membranes. In low ionic strength thick dense fibrils form large networks, which coexist with amorphous aggregates. High ionic strength results in less compact fibrils, that assemble in large sheets packed with globular PrP particles, resembling diffuse aggregates found in ex vivo preparations of PrP^{Sc}. Here we report on the finding of a β-turn-rich conformation involved in prion fibrillization that is toxic to neuronal cells in culture. This is the first account of an intermediate in prion fibril formation that is toxic to neuronal cells. We propose that this unusual β-turn-rich form of PrP may be a precursor of PrP^{Sc} and a candidate for the neurotoxic molecule in prion pathogenesis.

Keywords: Prion conversion; Rafts; Fibrillization; Transmissible spongiform encephalopathy; Neurotoxic molecule

Deposition of amorphous protein aggregates and amyloid fibrils in different organs of the human body and other animals is a common feature of a wide range of diseases, including systemic amyloidosis, diabetes, Alzheimer's, Parkinson's, and transmissible spongiform encephalopathies (TSEs) [1]. In these diseases a key protein undergoes a major conformational change from its cellular normal structure to an alternative state, which forms amorphous and/or fibrillar aggregates. In most cases this transformation involves a partial unfolding of the native state and refolding into a β-sheet-rich conformation.

TSEs include Creutzfeldt–Jacob disease (CJD) in humans, bovine spongiform encephalopathy (BSE), scrapie in sheep, and chronic wasting disease (CWD) in deer and elk, amongst others. *Prion* is the key protein associated with the pathogenesis of TSEs and is the major component of amyloid plaques and amorphous protein deposits found in the brains of deceased patients and laboratory animals or in cell culture models. In normal healthy conditions prion is a harmless plasma membrane protein predominantly expressed in the brain and implicated in copper binding and cell signaling [2–4].

☆ *Abbreviations:* AFM, atomic force microscopy, ATR FTIR, attenuated total reflection Fourier transform infrared; CD, circular dichroism; chol, cholesterol; DPPC, dipalmitoylphosphatidylcholine (1,2-dipalmitoyl-*sn*-glycero-3-phosphocholine); EM, electron microscopy; PrP, prion protein; MTT, 3-(4,5-dimethylthiazol-2-yl)-2,5-diphenyltetrazolium bromide; NMR, nuclear magnetic resonance; SHaPrP, Syrian hamster prion protein; SM, sphingomyelin.

* Corresponding author. Fax: +44 24 7652 3701.
E-mail address: t.pinheiro@warwick.ac.uk (T.J.T. Pinheiro).

0006-291X/$ - see front matter © 2005 Elsevier Inc. All rights reserved.
doi:10.1016/j.bbrc.2004.12.172

Prion is a 209-amino acid long protein, with two N-glycosylation sites at asparagines 147 and 198 (hamster PrP numbering is used throughout this article) and incorporated in the outside face of the cell membrane via a glycosylphosphatidylinositol (GPI) lipid anchor coupled to Ser 231 at the C-terminus [5]. Prion also contains two cysteine residues (Cys 197 and 214), which form an intramolecular disulfide bond that provides structural stability to the C-terminal domain of the protein.

A key molecular event in TSEs is the conversion of the normal cellular form of the prion protein (PrP^{C}) to the aberrant amyloid form, generally denoted as scrapie isoform (PrP^{Sc}). The molecular details of this transformation are not fully understood, but it appears to involve a partial unfolding of the monomeric cellular form and subsequent refolding into an oligomeric aggregated or fibrillar form. High-resolution NMR structures of different constructs of PrP^{C} exist for most prion species [6], showing that PrP^{C} is rich in α-helical structure (47%), has a long unstructured N-terminus comprising nearly half of the amino acid sequence, and a small amount of antiparallel β-sheet (3%). In contrast, a high-resolution structure for PrP^{Sc} remains elusive, but low-resolution structure analysis revealed that PrP^{Sc} is enriched in β-sheet [7,8] and electron crystallography-derived models support a parallel left-handed β-helical fold for PrP^{Sc} in 2D crystals that co-purify with prion amyloid rods [9,10]. Because of the multiple forms and lengths of PrP^{Sc}, and inherent difficulties of structure determination on aggregated, sometimes impure PrP^{Sc} extracts, values for the secondary structure content of PrP^{Sc} vary. Reported values for the α-helix content are found within the range 17–30% and for β-sheet structure within 43–54% [7,8].

Accumulation in the brain of prion aggregates and fibrillar assemblies is normally associated with spongiform degeneration and neuronal death [11–13]. However, the mechanism how prions damage cells and the precise nature of the neurotoxic molecule in prion diseases are not fully understood [14]. Due to the insolubility of ex vivo preparations of PrP^{Sc}, only a few studies have tested directly the neurotoxicity of PrP^{Sc} to neurons in culture [15–17]. However, the results are difficult to interpret, because of the uncertainties about the physical state of PrP^{Sc}. Most neurotoxicity studies of PrP employ synthetic peptides derived from the PrP sequence [18], and none have been reported for β-sheet-rich forms, produced in vitro, of the full-length PrP(23–231) or the truncated protein PrP(90–231).

In order to decipher the structural details of PrP conversion, in vitro studies of fibrillization and aggregation of recombinant prion proteins are very useful. Recombinant PrP can be refolded as an α-helical-rich form (α-PrP) corresponding to PrP^{C} and β-sheet-rich forms (β-PrP) with properties of PrP^{Sc} [19,20]. Studies of fibril formation with α-PrP have shown that the morphology of aggregates and fibrils depends on partial unfolding of PrP, salt concentration, and pH [21–23]. In an earlier work, we reported that a β-PrP can more readily form fibrils in raft membranes, compared to α-PrP [24]. Here we present the characteristics of fibrillization of β-PrP under partial denaturing conditions and in raft membranes, and reveal unusual structural properties of early aggregates in the fibrillization of PrP. The potential significance of these early states in prion neuropathogenesis is postulated from their observed cytotoxic effects on neuronal cells.

Materials and methods

Expression, purification, and refolding of PrP. Syrian hamster recombinant prion protein SHaPrP(90–231) was expressed using an alkaline phosphatase promoter in a protease-deficient strain of *Escherichia coli* (27C7) as described previously [25]. The prion protein accumulates as insoluble aggregates in the periplasmic space. From these inclusion bodies PrP can be refolded to a predominantly α-helical conformation (α-PrP) or to a state with a higher content of β-sheet structure (β-PrP), depending on whether refolding is carried out under oxidizing or reducing conditions, respectively [25,26]. Purification of α-PrP was carried out as described in Sanghera and Pinheiro [27], and β-PrP was prepared according to the method mentioned in Kazlauskaite et al. [24]. Purified PrP was dialyzed against 5 mM Mes, pH 5.5, for α-PrP and, pH 6.5, for β-PrP and stored in small aliquots. Protein samples were thawed prior to measurements and used on the same day, unless stated otherwise. PrP concentration was determined spectrophotometrically using a molar extinction coefficient ε_{280} of 24,420 $M^{-1}\,cm^{-1}$ [28].

Lipid vesicles. Cholesterol and sphingomyelin were purchased from Avanti Polar Lipids (Alabaster, AL). DPPC was from Sigma–Aldrich (Dorset, UK). Small unilamellar lipid vesicles were prepared as reported previously [24]. Briefly, for the preparation of mixed lipid membranes the required amounts of lipids were co-dissolved in chloroform and dried in a rotary evaporator. The resulting lipid film was left under vacuum overnight to remove all traces of organic solvent. The dried lipid was hydrated with the required buffer: 2 mM Mes, pH 5 or 7. Buffers were deoxygenated with nitrogen gas and hydrated lipids were stored under nitrogen atmosphere. After lipid hydration the resulting multilamellar suspension was sonicated in a bath sonicator until a clear suspension of small unilamellar vesicles was obtained (typically six 1/2 h periods).

Infrared spectroscopy. Attenuated total reflection (ATR) Fourier transform infrared (FTIR) spectra were recorded at room temperature on a Bruker Vector 22 infrared spectrometer equipped with a liquid nitrogen-cooled mercury cadmium telluride (MCT) detector at a nominal resolution of 4 cm^{-1} in the range 1000–4000 cm^{-1}. The spectrometer was continuously purged with dried air (Jun-Air 600; Kent, UK) to minimize the spectral contribution from atmospheric water. Residual water vapor peaks were subtracted using reference spectra and baseline correction was applied when necessary. The internal reflection element was a germanium ATR plate (50 × 20 × 2 mm) with an aperture angle of 45° yielding 25 internal reflections.

Typically, an aliquot of 20–50 μl of samples containing 4.5 to 27 μM protein in buffer solution was deposited on the ATR plate and a thin hydrated protein film was obtained by slowly evaporating the excess water under a stream of N_2 gas. High molecular weight aggregates of β-PrP were separated from smaller oligomers by ultracentrifugation at 391,000*g* at 4 °C for 1 h. Lipid–protein samples were prepared by the addition of an aliquot of a stock solution of β-PrP in 5 mM Mes buffer, pH 5.5, to preformed lipid vesicles in 2 mM Mes buffer, pH 5. Samples normally contained 10 μM PrP and 0.1–10 mM lipid, and an aliquot of 40 μl deposited on the ATR plate. Thin films of hydrated multibilayers of lipid containing PrP are formed by slowly

evaporating the excess water under a stream of N_2 gas. This procedure results in stacks of orientated bilayers with the lipid acyl chains approximately perpendicular to the surface of the plate [29]. Typically, the final spectrum is an average of 256 scans, corrected for the background using a clean germanium plate.

All ATR FTIR spectra were collected after a short period of H_2O/D_2O exchange in order to aid the analysis of protein secondary structure [30,31]. Deposited films on the ATR plate, prepared from samples in H_2O, were subjected to a stream of D_2O-saturated N_2 gas for 30 min at room temperature. Peak fitting of the amide I band (1600–1700 cm^{-1}) was performed on non-deconvoluted spectra using GRAMS 32/AI software (Thermogalactic, USA). Best fits to the experimental spectra were obtained with a Lorentzian lineshape with a full width at half height 5–6 cm^{-1}. Band assignments were made according to Cabiaux et al. [32], helped by second derivative analysis of the FTIR spectra when necessary.

Circular dichroism. Far-UV (185–260 nm) CD spectra were measured on a JASCO J-715 spectropolarimeter using 1-mm-pathlength quartz cells. Typically, a scanning rate of 100 nm min^{-1}, a time constant of 1 s, a bandwidth of 1.0 nm, and a resolution of 1 nm were used. Spectra were measured at 20 ± 0.2 °C on samples containing 4.5 (supernatant), 27 (pellet), and 21 μM (total sample) protein in 2 mM Mes buffer, pH 6.5. Typically 16 scans were averaged per spectrum and the background buffer was subtracted from the final spectra.

Cell culture. PC12 neuroblastoma cells (rat pheochromocytoma, American Type Culture Collection) were cultured in RPMI medium (Gibco-BRL) supplemented with 5% fetal bovine serum, 3 mM glutamine, 100 U ml^{-1} penicillin, and 100 μg ml^{-1} streptomycin in a 5% CO_2-humidified atmosphere at 37 °C. Cells were plated at a density of 8000 cells per well on 96-well plates in 80 μl of fresh medium. After 24 h, 20 μl PrP (0.01–0.1 μM) was added to the wells. Cell viability was evaluated 1–4 days later through the reduction assay of 3-(4,5-dimethylthiazol-2-yl)-2,5-diphenyltetrazolium bromide (MTT). Production of blue formazan upon reduction of MTT by mitochondrial succinate dehydrogenase was measured by recording the absorbance values at 590 nm with an automatic plate reader.

Electron microscopy. Stock solutions of β-PrP in 2 mM Mes buffer, pH 6.5, were used for the EM measurements of fibrillization. Denaturant or salt was added to the protein as a small aliquot from a high concentrated stock solution. Samples were diluted to a protein concentration ~150 μg ml^{-1}, applied to electron microscope grids coated with carbon film, and stained with 2% uranyl acetate. The preparations were examined using a Philips CM120 electron microscope with an accelerated voltage of 100 kV. Electron micrographs were taken at a magnification of 45,000 under low dose conditions. Lipid–protein samples were prepared as described before [24].

Atomic force microscopy. Typically, an aliquot of 10 μl of protein solution (containing 80–150 μg ml^{-1} of protein) with or without denaturant was deposited onto a glass coverslip, allowed to dry overnight, and then rinsed with water to remove denaturant. Excess water was removed with a gentle stream of compressed air. AFM images were acquired on a Digital Instruments Multimode AFM operated by a Nanoscope IIIa controller, using a model E scanner capable of a maximum scan range of 10 × 10 μm. Images were recorded in tapping mode using a single beam silicon cantilever; nominal resonant frequency ~300 kHz at scan rates of 1 and 1.5 Hz.

Results

Structural properties of β-PrP

PrP(90–231) can be refolded from *E. coli* inclusion bodies either as an α-helical conformation (α-PrP) or a state with a higher content of β-sheet structure (β-PrP). Refolding under oxidizing conditions yields the α-PrP isoform which shows a characteristic far-UV CD spectrum with well-defined minima at 208 and 222 nm (data not shown) [24], and a FTIR spectrum with a predominant amide I band ~1646 cm^{-1} (Fig. 1A). In contrast, refold-

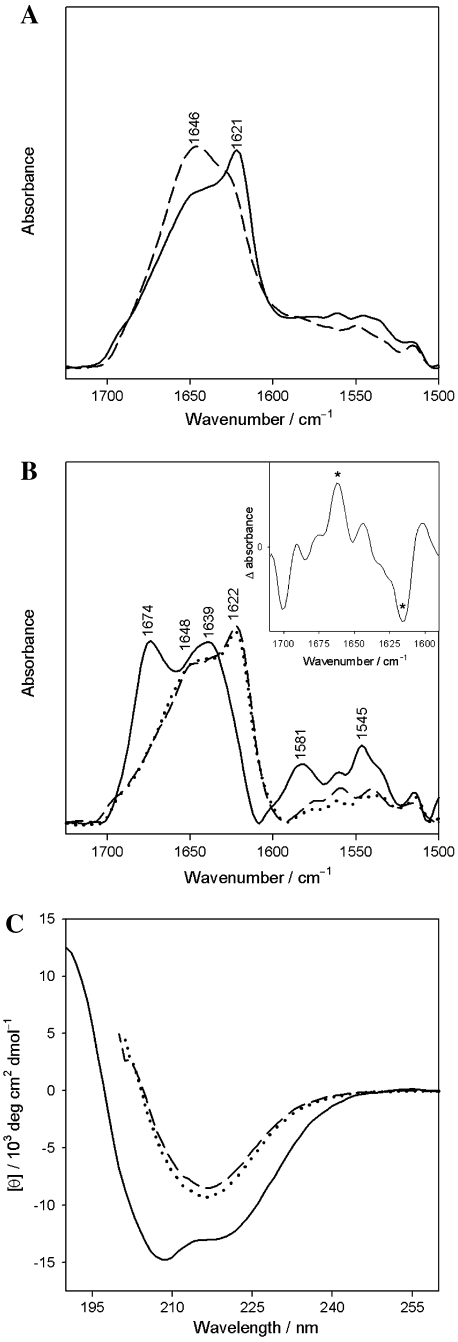

Fig. 1. ATR FTIR spectra of (A) α- and β-isoforms of PrP(90–231) freshly refolded from *E. coli* inclusion bodies (solid line, β-PrP; dashed line, α-PrP) and (B) 1-month-old β-PrP (dotted line, total protein; dashed line, pellet; and solid line, supernatant). Inset shows the difference spectrum of β-PrP total minus pellet. (C) Far-UV CD spectra of total β-PrP (dotted line), clear pellet (dashed line), and supernatant (solid line). ATR FTIR spectra were collected after a short period of H_2O/D_2O exchange (see Materials and methods).

ing of PrP(90–231) under reducing conditions produces a β-PrP isoform which shows a far-UV CD spectrum with a minimum ~217 nm (data not shown) [24] and an intense amide I band ~1621 cm^{-1} (Fig. 1A), which are spectral properties of β-sheet structure.

The α-PrP isoform is monomeric and fully degraded by proteinase K, whereas β-PrP tends to be oligomeric, forms insoluble amorphous aggregates and fibrils, and is more resistant to proteinase K digestion (data not shown). Attempts to identify the oligomeric states of β-PrP by analytical gel filtration were difficult but informative. Elution of β-PrP under native conditions, in the absence of denaturant or high salt concentrations, revealed that only 6–8% of the protein elutes from the column. Under other conditions, i.e., varying concentrations of NaCl (10–100 mM) and different pHs (4–6.5) dimeric, tetrameric, and octameric, as well as higher oligomeric forms of PrP, could be eluted at recovery yields of around 15% (data not shown). The low protein recovery from the gel filtration column indicates that β-PrP is highly hydrophobic and/or contains large aggregates. These experiments show that β-PrP exists in diverse conformations and oligomeric states, with the proportion and occurrence of the various states depending on the experimental conditions, in agreement with previous reports [20,21,33].

High molecular weight aggregates and oligomers of β-PrP can be separated from smaller forms by ultracentrifugation. Stock solutions of β-PrP at concentration ~80 μM (1.3 $mg\,ml^{-1}$) form clear solutions but after ultracentrifugation a pellet is separated from the supernatant. FTIR analysis of an aliquot collected from the bottom of the tube shows a spectrum with a strong amide I band ~1622 cm^{-1} nearly indistinguishable from the spectrum of total protein (Fig. 1B) and corresponding far-UV CD spectra show a broad negative dichroic band around 217 nm for both total and pelleted proteins (Fig. 1C). Both the FTIR and CD spectra indicate a high content of β-sheet structure in the species pelleted by ultracentrifugation. In contrast, the species remaining in the supernatant are highly α-helical, as shown by the typical CD spectrum with two minima at 208 and 222 nm (Fig. 1C). Similarly, the FTIR spectrum does not show a pronounced peak for β-sheet structure, but an amide I with intensities at 1639 and 1648 cm^{-1}, associated with random coil, and α-helix, respectively, and a distinct peak at 1674 cm^{-1} (Fig. 1B) assigned to solvent-exposed C=O group of β-turns [34]. In addition, the spectrum of species in the supernatant has higher intensity in the region 1590–1510 cm^{-1}, which is associated with absorbance of amino acid side chains.

Protein analysis showed that the species remaining in the supernatant can account for up to ~40% of the total protein. The difference between the spectrum of total sample minus that of pellet shows an intense positive peak for β-turns ~1662 cm^{-1} and a strong negative peak for β-sheet ~1615 cm^{-1} (Fig. 1B, inset), which reflect the spectral contributions identified for the species in the supernatant. This observation indicates that the species separated in the supernatant coexist with larger aggregates in the total sample and are not a result of the ultracentrifugation procedure.

Quantitative analysis of the amide I band yields the content of secondary structure for the different species in the supernatant and pellet, and is compared to freshly refolded α- and β-PrP isoforms. The α-PrP isoform has 43% α-helix, 25% random coil and 19% β-sheet, in good agreement with the NMR structure [35]. The β-PrP form has a lower content of α-helical structure (17%) and a high content of β-sheet (35%). The secondary structure content of β-PrP is overall analogous to the secondary structure of the proteinase K-resistant core of PrP extracted from tissues of diseased animals [7]. The structure of β-PrP, kept at −20 °C in Mes buffer, pH 5, at concentrations ~1 $mg\,ml^{-1}$, changes with time. After thawing (once) and ultracentrifugation, pelleted aggregates from β-PrP solutions show increasing levels of β-sheet structure with time, reaching 48% by six months. In contrast, soluble species remaining in the supernatant have reduced β-sheet (26%), elevated α-helix (29%), and an unusually high content of β-turns (45%), relative to freshly refolded β-PrP.

Fibrillization of β-PrP in solution

Solutions of β-PrP tend to form small aggregates, particularly at neutral pH, which can be observed by EM [24]. Initially, these aggregates are globular with a diameter of ~15–20 nm. Over time, solutions of β-PrP stored at −20 °C, at protein concentrations ~80 μM, are found to contain larger aggregates. These aggregates have the appearance of worm-like curved particles of an average length of 40 nm and a diameter ~10 nm (Fig. 2A). These particles are typically observed during the early stages of fibril formation of amyloidogenic proteins and are known as protofibrils [36–38]. The largest particles can reach 75 nm in length and some smaller, round oligomers appear to have an annular shape (Fig. 2A, arrows). Globular particles with a central channel are associated with the earliest protofibrillar precursors and have been observed with other amyloid proteins [37,39,40].

Addition of low concentration of denaturant (0.5 M GdnHCl) to these protofibrillar solutions of β-PrP allowed us to capture an early stage in the fibrillization process of PrP, where small globular aggregates appear to rapidly assemble into long and thin filaments (Fig. 2, transition from A to B). This remarkable transition occurs in less than 5 min, resulting in early assemblies of narrow filaments with diameters around 10 nm and maximum lengths of 3–4 μm, which are seen to twist around each other to form thicker bundles comprising

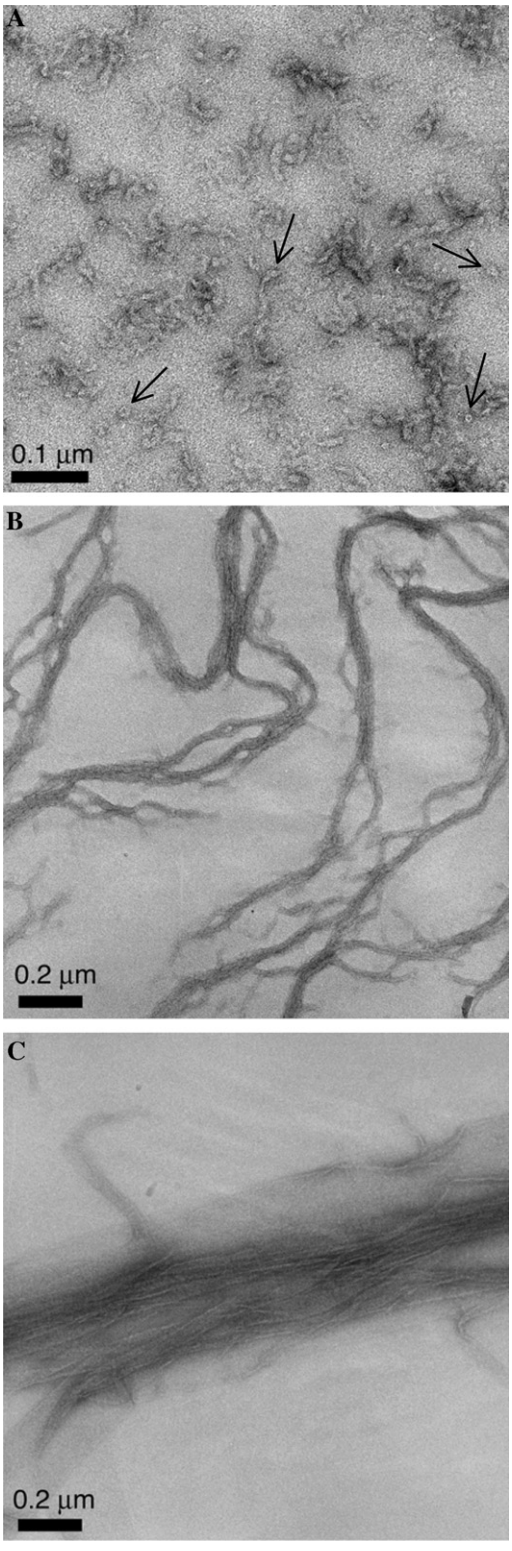

Fig. 2. Electron microscopy images of negatively stained β-PrP in (A) buffer solution, (B) immediately after addition of 0.5 M GdnHCl and (C) 24-h later. Arrows in (A) highlight annular oligomers.

2–25 filaments. After 24 h the samples are found to contain a mixture of sheet-like structures (suggesting a fusion of filaments), ribbon-like structures, and filaments

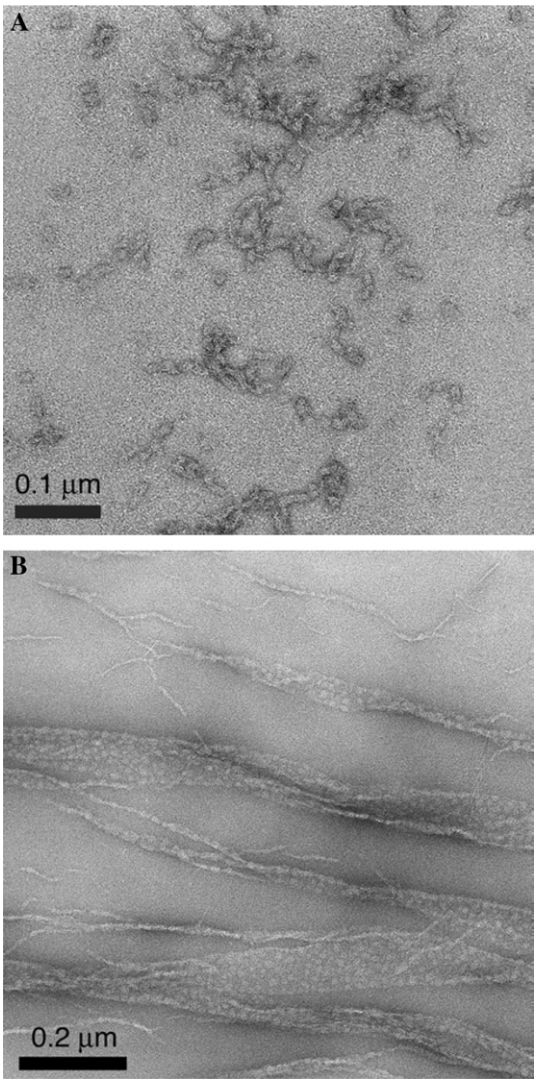

Fig. 3. Electron microscopy images of negatively stained β-PrP in the presence of (A) 50 mM NaCl and (B) 200 mM NaCl and 1 M GdnHCl after 24 h at room temperature.

that do not appear to form bundles but are rather loosely associated with each other (Fig. 2C). The width of the largest bundles comprising sheets, ribbons, and loosely associated filaments can reach 0.5 μm.

Addition of NaCl alone (in the absence of denaturant) to β-PrP solutions results in protofibrillar structures (Fig. 3A), but addition of NaCl and denaturant results in rapid formation of ribbons (Fig. 3B) that can loosely associate with each other to form less packed bundles than those observed in the absence of NaCl. These ribbon structures have a maximum width of 150 nm and can reach lengths of 8 μm. As with the sheets formed in the absence of NaCl (Fig. 2C), ribbons appear to be packed with smaller globular particles (Fig. 3B). The EM images show that filaments formed in partial denaturing condition with GdnHCl are flat assemblies, with a ribbon- or sheet-like morphology, where small protein granules appear to pack in a two-dimensional layer.

Packing of the oligomeric aggregates within the ribbons and association of ribbons into bundles appears to become weaker in the presence of NaCl.

Using the non-ionic denaturant, urea, in the absence of NaCl, a different morphology of fibrils and kinetics of fibrillization were observed. Addition of 1 M urea to β-PrP solutions first results in the formation of diffuse aggregates of PrP (Fig. 4A), which persist over hours, in contrast with the rapid assembly of fibrils in GdnHCl. With time these aggregates slowly form filaments that assemble into dense, thick fibrils with gentle twists along the fiber (Fig. 4B). Fibrils formed in urea develop more slowly than in GdnHCl and appear to be assembled from thin filaments of about 10 nm in width into denser, thicker fibrils reaching 300 nm in width. By 26 h a crowded network of thick, dense fibrils is observed (Fig. 4B, inset).

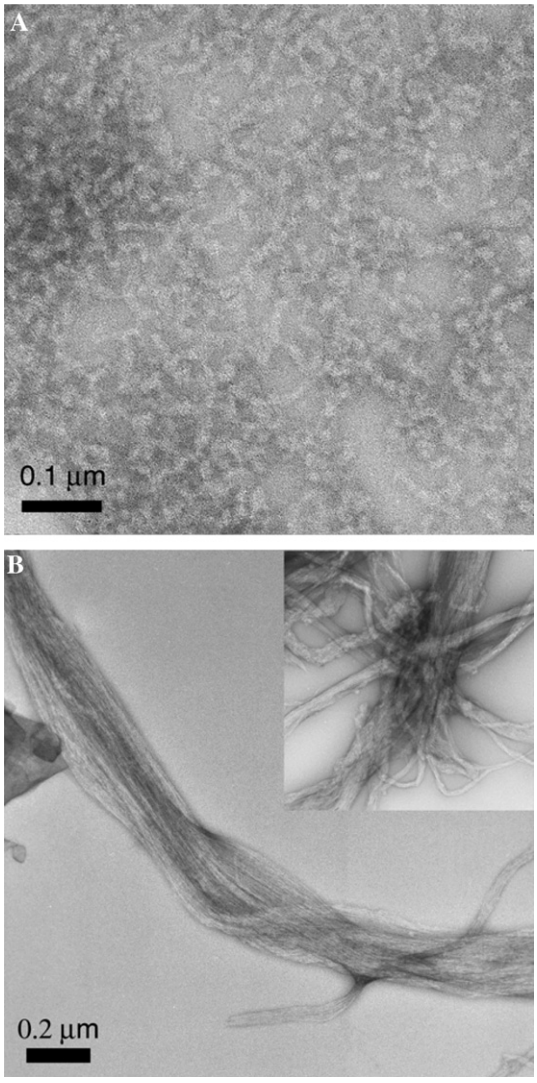

Fig. 4. Electron microscopy images of negatively stained β-PrP in the presence of 1 M urea after (A) 2 and (B) 26-h incubation. Inset (B) shows the dense network of fibrils observed at 26 h.

Atomic force microscopy (AFM) of β-PrP samples revealed a population of needle-like straight aggregates of average length ~50 nm and width ~10 nm (Fig. 5A), which remains in the supernatant after ultracentrifugation. Similar needle-like structures have been reported for α-synuclein in AFM fibrillization studies and are also classified as protofibrils [41]. In agreement with

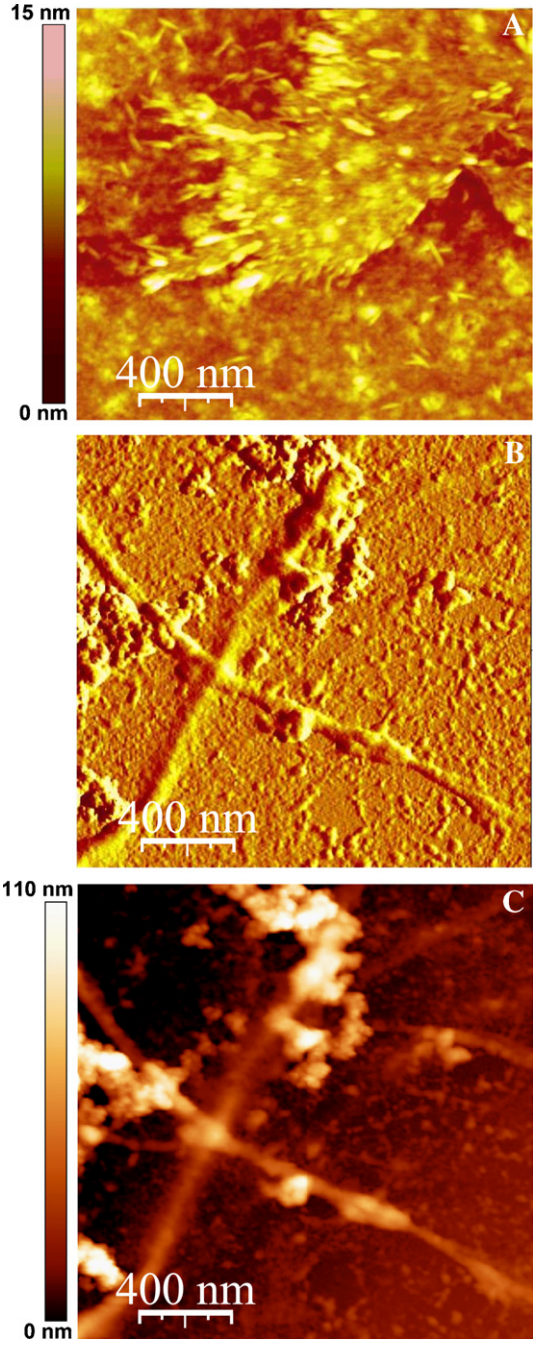

Fig. 5. Tapping mode atomic force microscopy images of β-PrP in buffer solution showing (A) needle-like aggregates and (B,C) fibrils formed in the presence of 1 M urea after one week incubation at room temperature. Images in amplitude (B) and topographic (C) modes illustrate a large network of fibrils with aggregates. Height scales are shown on the left of topographic panels.

the EM results, fibrils formed in the presence of urea were also seen under AFM to be assembled from thin and long filaments that twist around each other (Fig. 5B) and were found to form large networks in association with amorphous aggregates (Fig. 5C).

High concentrations of salt or denaturants interfere with ATR FTIR measurements. Binding of thioflavin T (ThT) is commonly used to assess fibril formation, due to its enhanced fluorescence when bound to amyloid proteins rich in β-sheet structure. Thus, β-sheet-rich states during fibrillization of proteins are often identified from ThT binding measurements. ThT does not bind to the α-PrP isoform, showing a negligible level of fluorescence background at around 480 nm. A 3.5-fold increase in ThT fluorescence was observed when ThT is added to β-PrP, consistent with the higher level of β-sheet structure. Protofibrils formed by the addition of NaCl (Fig. 3A) show a 5.5-fold increase in ThT fluorescence relative to the background level of ThT fluorescence in the presence of α-PrP, and fibrils formed with 0.5 GdnHCl show an 8.5-fold increase in ThT fluorescence (data not shown). The changes in ThT fluorescence corroborate the fibrillar nature of the assemblies seen under EM and AFM, and are consistent with the expected high content of β-sheet structure in protofibrils and fibrils.

Fibrillization of β-PrP in lipid membranes

Binding of β-PrP to model raft membranes composed of DPPC/chol/SM (50:30:20, molar ratio) induces a partial unfolding of PrP [24] and after 3 weeks protofibrils are found in these preparations (Fig. 6A), in contrast to incubations of α-PrP with raft membranes where no aggregation or fibrillization of PrP was observed. Binding of β-PrP to raft membranes results in a reduction of β-sheet and a large increase in random coil, from 4% in solution to 39%, with no significant change in α-helix content. These structural changes were observed immediately after binding β-PrP to raft vesicles [24]. Here we report the structure of β-PrP over the incubation period leading to the formation of protofibrils in raft membranes. FTIR spectra were collected over the time course of three weeks and the progress of structural changes is highlighted in Fig. 6B. Initially, the changes are very slow. Only by the end of the first week can spectral changes be noticed, including a marked increase of the band at 1674 cm^{-1} and reduction of the component ~1644 cm^{-1} (Fig. 6B). Peak fitting analysis revealed that over the 3-week period the main changes are a significant reduction in the random coil (spectral intensity ~1644 cm^{-1}) from 39% to 10%, with a parallel increase in β-turns (band at 1674 cm^{-1}) from 18% to 45%. The β-turn content of protofibrils formed in raft membranes is similar to that in protofibrils isolated in the supernatant of β-PrP solutions. In addition, simultaneous to the increase in β-turns there is a prominent gradual appearance of bands in the region between 1590 and 1510 cm^{-1} (Fig. 6B), which is associated with absorbance of amino acid side chains [42].

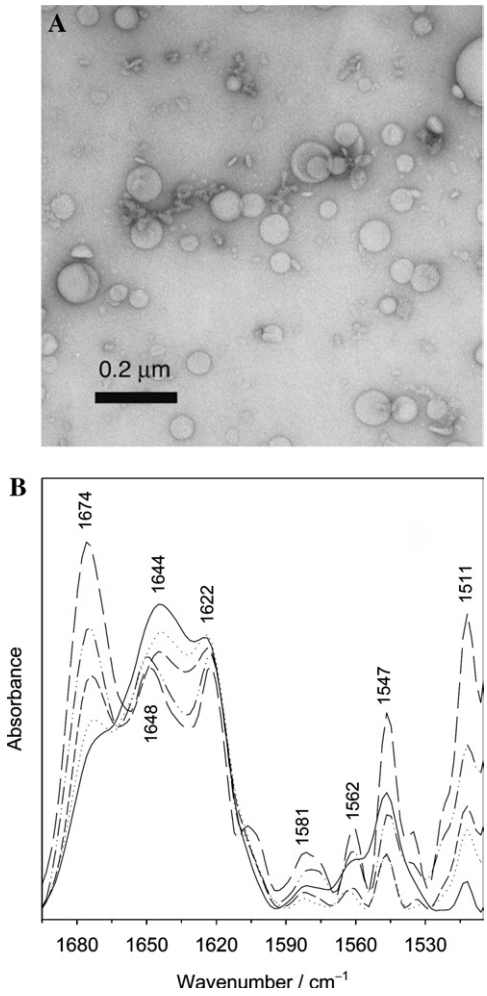

Fig. 6. (A) Electron microscopy image of negatively stained β-PrP protofibrils formed in the presence of raft vesicles composed of DPPC/chol/SM (50:30:20, molar ratio) at pH 5. Circular structures are vesicles. (B) Representative ATR FTIR spectra of β-PrP with raft vesicles showing the main structural changes over an incubation period of 3 weeks leading to the formation of protofibrils shown in (A). Freshly prepared sample (solid line), 8 (dotted line), 11 (short dash), 14 (dash-dot-dot), and 21 days (long dash).

Neurotoxicity of β-PrP aggregates

Recent studies with amyloidogenic proteins, including proteins not associated with disease, revealed that pre-fibrillar assemblies (protofibrils and small oligomers) have the highest cytotoxicity to cultured cells, whereas mature fibrils are less toxic or even harmless [39,40,43,44]. Although oligomers and protofibrils of PrP have been observed during in vitro fibrillization studies [19–21,45], it is not known if such aggregates are neurotoxic. We have tested the cytotoxicity of β-PrP preparations and found that the β-sheet species

isolated in the supernatant that are rich in β-turns (Fig. 7A) have the highest cytotoxic effect on neuroblastoma cells compared to pelleted aggregates (Fig. 7B).

The dependence of cytotoxic effects on protein concentration is shown in Fig. 7C. Maximal effects are observed at 0.1 μM PrP. Relative to control measurements, α-PrP and β-PrP-pelleted aggregates isolated by ultracentrifugation have minimal cytotoxic effects on cells (~5% reduction in cell viability), whereas the β-turn-rich species of β-PrP that remain in the supernatant induce a 36% reduction in cell viability at 0.1 μM PrP. The cytotoxic effect decreases at higher protein concentration (Fig. 7C), which is consistent with the tendency of β-sheet forms of PrP to aggregate. The cytotoxicity of the prion neurotoxic segment PrP(106–126) to non-differentiated PC12 cells results in a reduction in cell viability of 20–35% at peptide concentrations of 100 μM or higher [46,47]. Using different cerebellar cell cultures, neurotoxic effects of PrP(106–126) achieve levels of 50% reduction in cell viability, at optimal concentrations of 80 μM peptide [48–50]. In comparison, the cytotoxicity we observe for the β-turn-rich species of β-PrP is a significant effect, inducing a 36% reduction in cell viability at a much lower protein concentration of 0.1 μM.

Discussion

A critical amount of β-sheet accelerates fibril formation

The conversion of the PrP^{C} to the PrP^{Sc} is a remarkable molecular event, involving a major refolding of α-helix and random coil in PrP^{C} to β-sheet structure in PrP^{Sc} [8]. Sporadic cases of prion diseases are associated with this extremely rare event of erratic folding of PrP^{C}, whereas in the infectious cases prion conversion appears to occur via a template-assisted mechanism, in which PrP^{C} is refolded by the interaction with PrP^{Sc} [51].

Previous studies have shown that recombinant PrP can be refolded as an α-helical conformation (α-PrP),

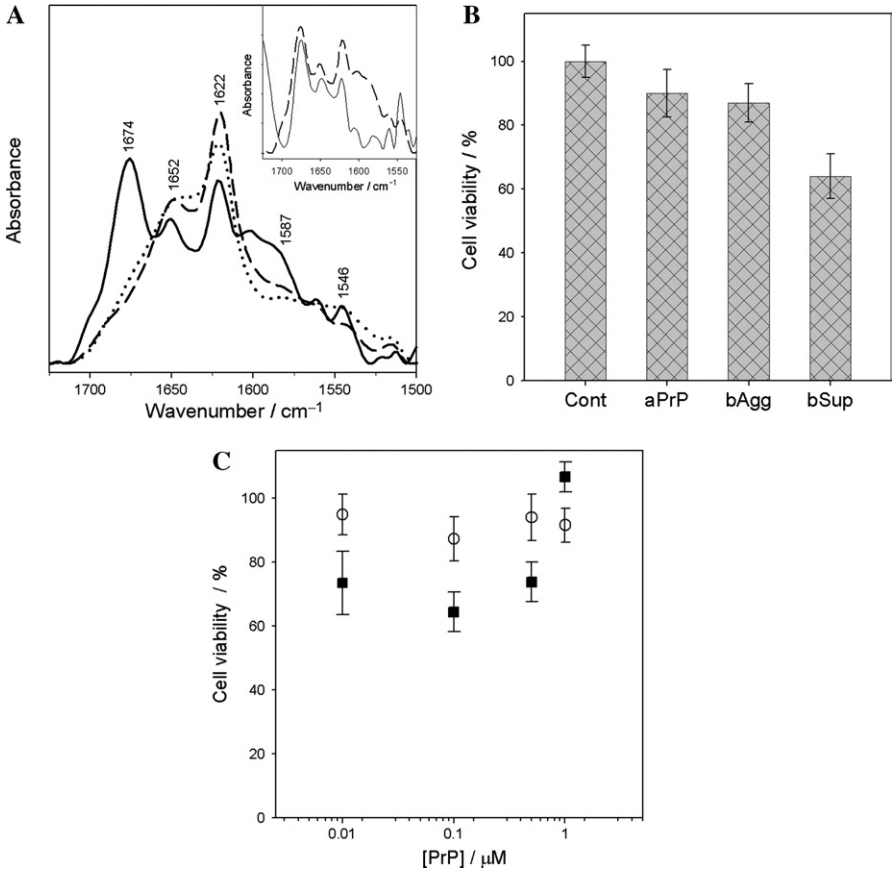

Fig. 7. (A) ATR FTIR spectra of 6-month-old β-PrP (dotted line, total protein; dashed line, pellet; and solid line, supernatant). Inset compares the amide I regions of the FTIR spectrum of supernatant species from 6-month-old β-PrP (dashed line) with that of β-PrP after 21-day incubation with raft vesicles (solid line). (B) Cytotoxic effects of β-PrP aggregates pelleted by ultracentrifugation (bAgg) and smaller species remaining in the supernatant (bSup) for 0.1 μM PrP concentration. For comparison the effects on cells treated with α-PrP (aPrP) are also shown at equivalent protein concentration (0.1 μM). Cell viability is measured as a percentage of MTT reduced by cells treated with PrP relative to MTT reduction by control cells (Cont) treated with buffer only (see Materials and methods). (C) The dependence of cytotoxic effects of β-PrP pelleted aggregates (circles) and supernatant species (squares) on PrP concentration. Cytotoxic effects were measured 24 h after addition of PrP and are an average of six wells per experiment.

representing PrP^C, which under a variety of conditions can be converted to aggregated and fibrillar forms rich in β-sheet, with physical properties resembling those of PrP^{Sc} [19,20,52]. These studies showed that fibrillization of α-PrP requires partial unfolding of PrP, provided by the presence of denaturants, such as GdnHCl or urea. Fibrillization of α-PrP can occur in hours to weeks, depending on conditions, including concentration of denaturant, pH, temperature, and presence of salts [19,22,23,45]. From these studies, it appears that a partially unfolded α-PrP is refolded into a β-sheet-rich state, which can either form amorphous aggregates or assemble into ordered fibrillar structures.

Recombinant PrP can also be refolded into β-sheet-rich oligomeric forms, with an intact, oxidized disulfide bond [20] or reduced cysteines [24,26,53]. The fibrillization studies we present here use a reduced, β-sheet-rich isoform of PrP (β-PrP, Fig. 1A). Although brain-extracted PrP^{Sc} has an intact disulfide bond [54], it is unclear whether disulfide reduction may play a role in prion conversion [53,55–57]. We show that β-PrP forms protofibrillar structures in the absence of any denaturants (Fig. 2A) and that addition of small amounts of denaturant leads to very rapid fibrillization (Fig. 2B). This fast assembly of PrP into fibrils has not been observed before in non-seeded fibrillization studies of α-PrP. The results suggest that prompt formation of PrP amyloid fibrils requires a loosely packed conformation of PrP with a critical amount of β-sheet.

The formation of amyloid fibrils is best described as a two-step reaction involving a nucleation step followed by a molecular assembly or polymerization phase [58,59]. Formation of a nucleus for polymerization and fibril growth appears to be the rate-limiting step. The current study shows that β-PrP forms protofibrils with characteristic ThT binding properties and high content of β-sheet (Figs. 1B and C). Similar protofibrillar structures have been reported for the α-helical form of PrP under acidic conditions in the presence of GdnHCl after 55-day incubation [45]. Here we show that fibril formation from β-PrP preparations is much faster (<5 min). Our results indicate that the nucleus for the polymerization of PrP must have a critical amount of β-sheet structure in order for fibril growth to proceed.

Amorphous aggregates and fibrils in solution and on membrane surfaces

In vivo, conversion of PrP^C to the disease-specific PrP^{Sc} results in insoluble fibrillar protein deposits, with the tinctorial and ultrastructural properties of amyloid [60], that are normally associated with non-fibrillar amorphous aggregates [61]. Despite a common fundamental architecture of amyloid fibrils [36], different morphologies of amyloid assemblies are observed under different fibrillization conditions, showing that variations in the protofibril organization occur under differing media. In addition, fibrils with different morphologies can be observed in the same preparation, which reflects the heterogeneity of ex vivo fibril extracts from tissues with amyloid deposits [62].

In our in vitro fibrillization studies of PrP different morphologies of fibrillar structures and aggregates are observed, depending on ionic strength and, possibly, on the original extent of destabilization of the starting conformation of PrP. Increasing ionic strength leads to less compact fibrils (Fig. 3 compared with Fig. 2), resulting in large sheets packed with globular protein aggregates. These assemblies closely resemble diffuse aggregates commonly observed in ex vivo preparations of PrP^{Sc}, where granular deposits of PrP are seen to organize in linear arrays and layers [63,64]. In contrast, thicker denser fibrils form in the presence of the non-ionic denaturant urea (Fig. 4). AFM results show that networks of fibrils coexist with amorphous aggregates (Figs. 5B and C). Association of β-PrP with raft membranes results in the formation of protofibrillar structures (Fig. 6A), which have been shown to grow into larger protofilaments from the vesicle surface [24]. Whether amorphous aggregates are recruited in fibril assembly has not been investigated in the present study; however, two studies with other proteins have shown that fibrils can be formed from amorphous aggregates [65,66].

PrP^C is associated with the outer surface of the plasma membrane via its GPI anchor, and like other GPI-anchored proteins, is segregated into cholesterol and sphingomyelin-rich domains, also known as lipid rafts [67]. The subcellular site for the formation of PrP^{Sc} is not clearly identified, but experimental evidence supports the plasma membrane and endocytic organelles as relevant sites [68–71]. We have shown in previous studies that the interaction of PrP with lipid membranes can lead to either amorphous aggregation or fibrillization of PrP, depending on the starting conformation of PrP and the lipid composition of the membrane [24,72]. The interaction of the α- or β-PrP isoforms with negatively charged lipid membranes results in increased β-sheet and the formation of amorphous aggregates. In contrast, raft membranes protect the α-helical conformation from aggregation, but binding of β-PrP results in partial unfolding and the formation of protofibrillar structures [24,27]. The strength of PrP association with membranes is also found to be pH-dependent, with β-PrP having in general a greater affinity to lipid membranes at pH 5 [73].

In the current study, the formation of PrP protofibrils in rafts was observed to be slower (over 3 weeks) than in solutions containing low amounts of denaturants (minutes to 2–3 days). We have shown previously that fibrillization of β-PrP is favored at pH 5 relative to pH 7 [24]. The results support our current view that the acidic

environment of endosomes and lysosomes not only contributes to a partial unfolding of PrP but also promotes a stronger association with the lipid membrane. The resulting membrane-associated altered conformation of PrP may have two main implications for the cellular cycle of PrP. Protein destined for degradation may become more resistant to proteolytic digestion and start to accumulate in the cell, forming aggregates. Alternatively, because PrP is constitutively recycled between endosomes and the plasma membrane [74], a corrupted conformation formed in endosomes can appear at the cell surface. A β-sheet-poised conformation of PrP has high affinity to rafts [24,73]. The accumulation of altered prion proteins in rafts facilitates protein-protein interactions, leading to the slow fibrillization of PrP on the membrane surface [72].

β-turns and exposure of side chains in fibril formation

FTIR analysis reveals that a loosely packed conformer of PrP with an unusually high level of β-turns is involved in the early stages of fibrillization of PrP (Fig. 1B). This β-turn-rich conformation of PrP is associated with smaller particles that remain in the supernatant after ultracentrifugation, which bind ThT (data not shown) and under AFM have the appearance of needle-like protofibrils (Fig. 5A). Similarly, protofibrils formed with raft membranes also show a high content of β-turns (Fig. 6). We propose that PrP protofibrils formed under solution conditions or in association with raft membranes are loosely packed structures, with high content of β-turns. In addition these protofibrillar assemblies have an unusually high absorbance in the FTIR spectrum between 1590 and 1510 cm^{-1} (Fig. 6B), consistent with exposure of side chains.

Exposure of side chains in PrP has recently been found to be associated with the pathologically misfolded prion conformation [75]. Antibodies directed to a repeat motif Tyr-Tyr-Arg recognize the pathological isoform of PrP but not the normal cellular form. During the fibrillization monitored in raft membranes (Fig. 6B), it is noteworthy that concurrent with the appearance of the β-turns band at 1674 cm^{-1} there is also a parallel development of side chain bands between 1590 and 1530 cm^{-1}. These bands have absorbance maxima typically associated with the side chains of aspartate, arginine, and glutamic acid [42], which in PrP(90–231) account for a total of 21 residues. In addition, it is very striking the progressive increase of the band at 1511 cm^{-1} associated with Tyr absorbance [42], which is in agreement with the exposure of the repeat motif Tyr-Tyr-Arg identified in the immunoprecipitation experiments by Paramathiotis et al. [75]. The authors also reported that the specific antibody binding to Tyr-Tyr-Arg motif in the pathological form of PrP could be reproduced in vitro to partially denatured normal brain prion protein. These findings are supported by our results with recombinant PrP. Furthermore, our results indicate that exposure of side chains is likely to be involved in the mechanism of fibrillization of PrP.

Exposure of side chains requires a partial unfolding of PrP, which is either provided by low amounts of denaturant, as in most of the reported fibrillization studies, or by lipid membranes [24]. This unfolding step in fibrillization appears to be a slow controlled process and more extensive unfolding is likely to result in aggregation. The slow unfolding step is a prerequisite to the slow nucleation step in amyloid formation, which in vitro is facilitated by the presence of destabilizing factors, such as denaturants, acidic pH, and interaction with lipid membranes. Thus, in vivo slow unfolding and formation of a crucial β-turn-rich nucleus could be the determinants in the observed long incubation times of prion diseases. Once a critical amount of these unusual species accumulates, very rapid fibril formation can occur, which fits the general characteristic of TSEs of very rapid clinical progression of patients after the onset of disease.

The finding that non-pathogenic proteins can form amyloid fibrils has led to the hypothesis that the potential to form amyloid may be a common property of all proteins [76]. In contrast to protein folding, which is driven by tertiary interactions between side chains or between side chains and backbone atoms, amyloid fibril formation is driven by backbone interactions, while side chain interactions work against fibril formation [77]. Our observations of unusual side chain absorbance fit this general mechanism, where side chain interactions in the native state must be destabilized and backbone interactions favored. Furthermore, our results show that simultaneous to side chain exposure there is a concomitant appearance of β-turn structure (Fig. 6B), which may serve as a precursor for fibril assembly and growth. In this scenario, the nucleus for PrP fibrillization would have a conformation rich in β-turns, which by an unknown mechanism unwinds and assembles into the β-sheet structure characteristic of amyloid fibrils. This transition of β-turns into β-sheet has been observed with synthetic oligopeptides [34], but further work is required to demonstrate that it can occur with proteins.

A cytotoxic conformation of PrP rich in β-turns

Accumulation of amyloid fibrils and other aggregates is a common feature of neurodegenerative diseases. In TSEs, prion fibrils and aggregates are normally associated with neuronal loss. A convergence of evidence supports the view that protein aggregation is neurotoxic and not a product of cell death [78]. However, the identity of the neurotoxic molecule and the mechanism by which it disables and eventually kills neurons are unknown [14]. Whilst a large fraction of the research on

prions has been focused in understanding the nature of the infectious agent, less attention has been given to the identification of the neurotoxic molecule. Moreover, it is suggested that the abnormal forms of PrP responsible for transmission and neuropathogenesis may be different [78].

Recently, it is has been found that protofibrils and small oligomers formed in the early stages of fibrillization of various amyloidogenic proteins, including proteins not involved in disease, have the highest cytotoxicity to cells in culture, whereas their mature fibrils are less toxic or harmless [39,40,43,44], but no studies have been reported as to the possible toxicity of early intermediates in prion fibril formation. These results have led to the proposal that the molecular basis of toxicity in amyloidosis may be related to the transient appearance of partially folded pre-fibrillar assemblies [79]. The accumulation of misfolded proteins inside or outside cells, due to their overproduction or disruption of the normal cellular clearance pathways, culminates in the formation of amorphous aggregates and amyloid fibrils. During this process precursor intermediates of fibrils and/or aggregates are formed that interfere with normal cellular pathways and incite cell death.

For TSEs there exists a growing perception that PrP^{Sc} aggregates and amyloid plaques are end products of the disease process and earlier PrP conformations are thought to be more relevant to the molecular mechanisms of neuropathogenesis and transmission [80,81]. In our present study, we have identified a soluble form of PrP involved in the early stages of fibril formation that is toxic to neuronal cells in culture (Fig. 7). This early intermediate is rich in β-sheet structure, and has an unusually high level of β-turns and exposed side chains. Our results show for the first time that β-sheet-rich species of PrP involved in the early stages of fibril formation are cytotoxic to cells. The finding adds the prion protein to a growing number of amyloid proteins for which their early pre-fibrillar assemblies (protofibrils and oligomers) have been shown to be more toxic than their corresponding mature fibrils. Our finding supports the suggestions that a precursor or by-product of PrP^{Sc} may constitute the neurotoxic molecule in prion diseases [14,78].

Although accumulation of PrP^{Sc} is commonly associated with the development of neuropathology, several situations have been described where this correlation is unclear, or where neurodegeneration occurs in the presence of low or undetectable levels of PrP^{Sc} (reviewed in [14]). In addition, areas of diseased brain with strong immunostaining for PrP^{Sc}, but with minimal or no neuropathological changes, can often be found. The evidence that neuropathology can develop in the absence of PrP^{Sc} and that PrP^{Sc} can accumulate without causing clinical symptoms argues that PrP^{Sc} itself might not be highly neurotoxic and other forms of PrP could be responsible for the prion-induced neurodegeneration. A potential candidate to fulfill this role would be an intermediate conformation of PrP in the conversion pathway from PrP^{C} to PrP^{Sc}. Such an intermediate has been hypothesized and referred to as PrP* [82].

The β-turn-rich conformation, identified in our current study, accumulates in preparations of β-sheet-rich isoform of PrP, in the absence of denaturant (Fig. 1), and on raft membranes (Fig. 6). This isoform promptly fibrillizes upon addition of small amounts of denaturant (Figs. 2–5) and is toxic to neuronal cells in culture (Fig. 7). This β-sheet isoform of PrP, rich in β-turns and with exposed amino acid side chains, has not previously been detected during fibrillization studies in vitro, because most of them employ partially denaturing conditions in the presence of salt and/or low amounts of denaturants. Under such conditions our β-sheet-rich PrP rapidly assembles into more compact structures, including diffuse aggregates (Figs. 2 and 3) and mature fibrils (Figs. 4 and 5). These assemblies resemble those observed in ex vivo preparations of PrP^{Sc} [63,64]. Moreover, partially misfolded PrP conformations with exposed side chains, associated with pathological conditions, have been detected in ex vivo brain extracts [75]. Therefore, it is plausible that the β-turn-rich species of β-PrP, identified in this study, could accumulate in vivo, especially in association with rafts at the plasma membrane, where formation of PrP^{Sc} is thought to occur.

The cytotoxic effects observed with our soluble β-turn-rich species of β-PrP are several orders of magnitude higher than the effects reported for the neurotoxic segment PrP(106–126) in similar measurements, as described in Results. This neurotoxic conformation of β-PrP involved in the process of aggregation and fibrillization of PrP may represent the hypothesized PrP* isoform and be a potential candidate for the neurotoxic molecule in prion pathogenesis. The rapid assembly of β-sheet isoforms of PrP observed in vitro suggests that in vivo such speedy response could provide a quick clearance mechanism of this highly toxic form of PrP. This process is driven by the physical properties of all protein sequences to form higher aggregates and amyloid fibrils when proteins are partially folded and expose their hydrophobic side chains. In sporadic TSEs, which constitute the majority of the cases of prion diseases (>80% of the total number of cases), aberrant partially folded forms of PrP may occur due to cellular changes associated with aging and degeneration of normal cellular pathways for the clearance of misfolded proteins.

A recent study showed that amyloid fibrils of recombinant prion protein, produced in vitro, are infectious to transgenic mice over-expressing PrP^{C} [83]. The results have re-ignited the debate on the nature of the infectious agent of prion diseases [84] and do not exclude the possibility of other forms of PrP having a role in prion neuropathogenesis and transmission, especially those

associated with early stages of aggregation and fibrillization of PrP. It remains to be established if other β-sheet-rich forms of PrP can also act as an infectious agent for prion diseases, and whether a common intermediate could be responsible for neuropathogenesis and transmission.

Acknowledgments

We thank Andrew Gill (IAH, Compton) for mass spectrometry analysis of prion proteins. Valuable comments on the manuscript were received from Andrew Gill (IAH, Compton), David Brown (University of Bath), and John Ellis (Biological Sciences, Warwick). This work has been supported by the Medical Research Council (G990445), the Biotechnology and Biological Sciences Research Council (88/BS516471), and the Royal Society. CV-B is funded by a Wellcome Trust project Grant (064775/Z01/Z).

References

[1] D.J. Selkoe, Folding proteins in fatal ways, Nature 426 (2003) 900–904.
[2] D.R. Brown, Role of the prion protein in copper turnover in astrocytes, Neurobiol. Dis. 15 (2004) 534–543.
[3] M.A. Prado, J. Alves-Silva, A.C. Magalhaes, V.F. Prado, R. Linden, V.R. Martins, R.R. Brentani, PrP^{C} on the road: trafficking of the cellular prion protein, J. Neurochem. 88 (2004) 769–781.
[4] X. Roucou, M. Gains, A.C. LeBlanc, Neuroprotective functions of prion protein, J. Neurosci. Res. 75 (2004) 153–161.
[5] N. Stahl, D.R. Borchelt, K. Hsiao, S.B. Prusiner, Scrapie prion protein contains a phosphatidylinositol glycolipid, Cell 51 (1987) 229–240.
[6] K. Wuthrich, R. Riek, Three-dimensional structures of prion proteins, Adv. Protein Chem. 57 (2001) 55–82.
[7] B.W. Caughey, A. Dong, K.S. Bhat, D. Ernst, S.F. Hayes, W.S. Caughey, Secondary structure analysis of the scrapie-associated protein PrP 27–30 in water by infrared spectroscopy, Biochemistry 30 (1991) 7672–7680.
[8] K.M. Pan, M.A. Baldwin, J. Nguyen, M. Gasset, A. Servban, D. Groth, I. Mehlhorn, Z. Huang, R.J. Fletterick, F.E. Cohen, S.B. Prusiner, Conversion of α-helices into β-sheet features in the formation of the scrapie prion proteins, Proc. Natl. Acad. Sci. USA 90 (1993) 10962–10966.
[9] H. Wille, M.D. Michelitsch, V. Guenebaut, S. Supattapone, A. Serban, F.E. Cohen, D.A. Agard, S.B. Prusiner, Structural studies of the scrapie prion protein by electron crystallography, Proc. Natl. Acad. Sci. USA 99 (2002) 3563–3568.
[10] C. Govaerts, H. Wille, S.B. Prusiner, F.E. Cohen, Evidence for assembly of prions with left-handed β-helices into trimers, Proc. Natl. Acad. Sci. USA 101 (2004) 8342–8347.
[11] S.J. DeArmond, W.C. Mobley, D.L. DeMott, R.A. Barry, J.H. Beckstead, S.B. Prusiner, Changes in the localization of brain prion proteins during scrapie infection, Neurology 37 (1987) 1271–1280.
[12] A. Williams, P.J. Lucassen, D. Ritchie, M. Bruce, PrP deposition, microglial activation, and neuronal apoptosis in murine scrapie, Exp. Neurol. 144 (1997) 433–438.
[13] M. Jeffrey, S. Martin, J. Barr, A. Chong, J.R. Fraser, Onset of accumulation of PrPres in murine ME7 scrapie in relation to pathological and PrP immunohistochemical changes, J. Comp. Pathol. 124 (2001) 20–28.
[14] R. Chiesa, D.A. Harris, Prion diseases: what is the neurotoxic molecule?, Neurol. Dis. 8 (2001) 643–763.
[15] W.E. Muller, H. Ushijima, H.C. Schroder, J.M. Forrest, W.F. Schatton, P.G. Rytik, M. Heffner-Lauc, Cytoprotective effect of NMDA receptor antagonists on prion protein (PrionSc)-induced toxicity in rat cortical cell cultures, Eur. J. Pharmacol. 246 (1993) 261–267.
[16] A. Giese, D.R. Brown, M.H. Groschup, C. Feldmann, I. Haist, H.A. Kretzschmar, Role of microglia in neuronal cell death in prion disease, Brain Pathol. 8 (1998) 449–457.
[17] K. Post, D.R. Brown, M. Groschup, H.A. Kretzschmar, D. Riesner, Neurotoxicity but not infectivity of prion proteins can be induced reversibly in vitro, Arch. Virol. Suppl. 16 (2000) 265–273.
[18] F. Tagliavini, G. Forloni, P. D'Ursi, O. Bugiani, M. Salmona, Studies on peptide fragments of prion proteins, Adv. Protein Chem. 57 (2001) 171–201.
[19] W. Swietnicki, M. Morillas, S.G. Chen, P. Gambetti, W.K. Surewicz, Aggregation and fibrillization of the recombinant human prion protein, Biochemistry 39 (2000) 424–431.
[20] I.V. Baskakov, G. Legname, M.A. Baldwin, S.B. Prusiner, F.E. Cohen, Pathway complexity of prion protein assembly into amyloid, J. Biol. Chem. 277 (2002) 21140–21148.
[21] B.-Y. Lu, J.-Y. Chang, Isolation of isoforms of mouse prion proteins with PrP^{Sc}-like structural properties, Biochemistry 40 (2001) 13390–13396.
[22] M. Morillas, D.L. Vanik, W.K. Surewicz, On the mechanism of α-helix to β-sheet transition in the recombinant prion protein, Biochemistry 40 (2001) 6982–6987.
[23] I.V. Baskakov, G. Legname, Z. Gryczynski, S.B. Prusiner, The peculiar nature of unfolding of the human prion protein, Protein Sci. 13 (2004) 586–595.
[24] J. Kazlauskaite, N. Sanghera, I. Sylvester, C. Vénien-Bryan, T.J.T. Pinheiro, Structural changes of the prion protein in lipid membranes leading to aggregation and fibrillization, Biochemistry 42 (2003) 3295–3304.
[25] I. Mehlhorn, D. Groth, J. Stockel, B. Moffat, D. Reilly, D. Yansura, W.C. Willett, M. Baldwin, R. Fletterick, F.E. Cohen, R. Vandlen, D. Henner, S.B. Prusiner, High-level expression and characterisation of a purified 142-residue polypeptide of the prion protein, Biochemistry 35 (1996) 5528–5537.
[26] H. Zhang, J. Stöckel, I. Mehlhorn, D. Groth, M.A. Baldwin, S.B. Prusiner, T.L. James, F.E. Cohen, Physical studies of conformational plasticity in a recombinant prion protein, Biochemistry 36 (1997) 3543–3553.
[27] N. Sanghera, T.J.T. Pinheiro, Binding of prion protein to lipid membranes and implications for prion conversion, J. Mol. Biol. 315 (2002) 1241–1256.
[28] S.C. Gill, P.H. von Hippel, Calculation of protein extinction coefficients from amino acid sequence data, Anal. Biochem. 182 (1989) 319–326.
[29] U.P. Fringeli, H.H. Günthard, Infrared membrane spectroscopy, Mol. Biol. Biochem. Biophys. 31 (1981) 270–332.
[30] E. Goormaghtigh, V. Cabiaux, J.-M. Ruysschaert, Secondary structure and dosage of soluble and membrane proteins by attenuated total reflection Fourier-transform infrared spectroscopy on hydrated films, Eur. J. Biochem. 193 (1990) 409–420.
[31] V. Raussens, V. Narayanaswami, E. Goormaghtigh, R.O. Ryan, J.-M. Ruysschaert, Hydrogen/deuterium exchange kinetics of apolipophorin-III in lipid-free and phospholipid-bound states, J. Biol. Chem. 271 (1996) 23089–23095.
[32] V. Cabiaux, R. Brasseur, R. Wattiez, P. Falmagne, J.-M. Ruysschaert, E. Goormaghtigh, Secondary structure of diphtheria toxin and its fragments interacting with acidic liposomes studied

by polarized infrared spectroscopy, J. Biol. Chem. 264 (1989) 4928–4938.
[33] G.S. Jackson, L.L.P. Hosszu, A. Power, A.F. Hill, J. Kenney, H. Saibil, C.J. Craven, J.P. Waltho, A.R. Clarke, J. Collinge, Reversible conversion of monomeric human prion protein between native and fibrillogenic conformations, Science 283 (1999) 1935–1937.
[34] H. Okabayashi, M. Ishida, H. Tamaoki, H. Masuda, C.J. O'Connor, Fourier transform IR study of aggregational behavior of *N*-acetyl-*l*- and *N*-butyloxycarbonyl-*l*-glutamic acid oligomeric benzyl esters in dioxane and benzene: β-turn → antiparallel β-sheet transition, Biopolymers 65 (2002) 129–141.
[35] T.L. James, H. Liu, N.B. Ulyanov, S. Farr-Jones, H. Zhang, D.G. Donne, K. Kaneko, D. Groth, I. Mehlhorn, S.B. Prusiner, F.E. Cohen, Solution structure of a 142-residue recombinant prion protein corresponding to the infectious fragment of the scrapie isoform, Proc. Natl. Acad. Sci. USA 94 (1997) 10086–10091.
[36] L.C. Serpell, M. Sunde, M.D. Benson, G.A. Tennent, M.B. Pepys, P.E. Fraser, The protofilament substructure of amyloid fibrils, J. Mol. Biol. 300 (2000) 1033–1039.
[37] H.A. Lashuel, B.M. Petre, J. Wall, M. Simon, R.J. Nowak, T. Walz, P.T. Lansbury Jr., α-Synuclein, especially the Parkinson's disease-associated mutants, forms pore-like annular and tubular protofibrils, J. Mol. Biol. 322 (2002) 1089–1102.
[38] M.A. Poirier, H. Li, J. Macosko, S. Cai, M. Amzel, C.A. Ross, Huntingtin spheroids and protofibrils as precursors in polyglutamine fibrilization, J. Biol. Chem. 277 (2002) 41032–41037.
[39] H.A. Lashuel, D.M. Hartley, B.M. Petre, J.S. Wall, M.N. Simon, T. Walz, P.T. Lansbury Jr., Mixtures of wild-type and a pathogenic (E22G) form of Aβ 40 in vitro accumulate protofibrils, including amyloid pores, J. Mol. Biol. 332 (2003) 795–808.
[40] M. Hoshi, M. Sato, S. Matsumoto, A. Noguchi, K. Yasutake, N. Yoshida, K. Sato, Spherical aggregates of β-amyloid (amylospheroid) show high neurotoxicity and activate tau protein kinase I/glycogen synthase kinase-3β, Proc. Natl. Acad. Sci. USA 100 (2003) 6370–6375.
[41] M.D. Shtilerman, T.T. Ding, P.T. Lansbury Jr., Molecular crowding accelerates fibrillization of α-synuclein: could an increase in the cytoplasmic protein concentration induce Parkinson's disease?, Biochemistry 41 (2002) 3855–3860.
[42] A. Barth, The infrared absorbance of amino acid side chains, Prog. Biophys. Mol. Biol. 74 (2000) 141–173.
[43] D.M. Walsh, I. Klyubin, J.V. Fadeeva, W.K. Cullen, R. Anwyl, M.S. Wolfe, M.J. Rowan, D.J. Selkoe, Naturally secreted oligomers of amyloid β-protein potently inhibit hippocampal long-term potentiation in vivo, Nature 416 (2002) 535–539.
[44] M. Bucciantini, E. Giannoni, F. Chiti, F. Baroni, L. Formigli, J. Zurdo, N. Taddei, G. Ramponi, C.M. Dobson, M. Stefani, Inherent toxicity of aggregates implies a common mechanism for protein misfolding diseases, Nature 416 (2002) 507–511.
[45] F. Sokolowski, A.J. Modler, R. Masuch, D. Zirwer, M. Baier, G. Lutsch, D.A. Moss, K. Gast, D. Naumann, Formation of critical oligomers is a key event during conformational transition of recombinant Syrian hamster prion protein, J. Biol. Chem. 278 (2003) 40481–40492.
[46] D.R. Brown, B. Schmidt, H.A. Kretzschmar, Effects of oxidative stress on prion protein expression in PC12 cells, Int. J. Dev. Neurosci. 15 (1997) 961–972.
[47] S. Onoue, K. Ohshima, K. Endo, T. Yajima, K. Kashimoto, PACAP protects neuronal PC12 cells from the cytotoxicity of human prion protein fragment 106–126, FEBS Lett. 522 (2002) 65–70.
[48] G. Forloni, N. Angeretti, R. Chiesa, E. Monzani, M. Salmona, O. Bugiani, F. Tagliavini, Neurotoxicity of a prion protein fragment, Nature 362 (1993) 543–546.
[49] D.R. Brown, M. Pitschke, D. Riesner, H.A. Kretzschmar, Cellular effects of a neurotoxic prion protein peptide are related to its β-sheet content, Neurosci. Res. Commun. 23 (1998) 119–128.
[50] M.F. Jobling, L.R. Stewart, A.R. White, C. McLean, A. Friedhuber, F. Maher, K. Beyreuther, C.L. Masters, C.J. Barrow, S. Collins, J.R. Cappai, The hydrophobic core sequence modulates the neurotoxic and secondary structure properties of the prion peptide 106–126, J. Neurochem. 73 (1999) 1557–1565.
[51] B. Caughey, G.J. Raymond, M.A. Callahan, C. Wong, G.S. Baron, L.W. Xiong, Interactions and conversions of prion protein isoforms, Adv. Protein Chem. 57 (2001) 139–169.
[52] W.Q. Zou, N.R. Cashman, Acidic pH and detergents enhance in vitro conversion of human brain PrP^{C} to a PrP^{Sc}-like form, J. Biol. Chem. 277 (2002) 43942–43947.
[53] N.R. Maiti, W.K. Surewicz, The role of disulfide bridge in the folding and stability of the recombinant human prion protein, J. Biol. Chem. 276 (2001) 2427–2431.
[54] E. Turk, D.B. Teplow, L.E. Hood, S.B. Prusiner, Purification and properties of the cellular and scrapie hamster prion proteins, Eur. J. Biochem. 176 (1988) 21–30.
[55] E. Welker, W.J. Wedemeyer, H.A. Scheraga, A role for intermolecular disulfide bonds in prion diseases, Proc. Natl. Acad. Sci. USA 98 (2001) 4334–4336.
[56] E. Welker, L.D. Raymond, H.A. Scheraga, B. Caughey, Intramolecular versus intermolecular disulfide bonds in prion proteins, J. Biol. Chem. 277 (2002) 33477–33481.
[57] S. Lee, D. Eisenberg, Seeded conversion of recombinant prion protein to a disulfide-bonded oligomer by a reduction–oxidation process, Nat. Struct. Biol. 10 (2003) 725–730.
[58] J.T. Jarrett, P.T. Landsbury Jr., Amyloid fibril formation requires a chemically discriminating nucleation event: studies of the amyloidogenic sequence from the bacterial OsmB, Biochemistry 31 (1992) 12345–12352.
[59] A. Lomakin, D.S. Chung, G.B. Benedek, D.A. Kirschner, D.B. Teplow, On the nucleation and growth of amyloid beta-protein fibrils: detection of nuclei and quantitation of rate constants, Proc. Natl. Acad. Sci. USA 93 (1996) 1125–1129.
[60] S.B. Prusiner, M.P. McKinley, K.A. Bowman, D.C. Bolton, P.E. Bendheim, D.F. Groth, G.G. Glenner, Scrapie prions aggregate to form amyloid-like birefringent rods, Cell 35 (1983) 349–358.
[61] S.J. DeArmond, S.B. Prusiner, Etiology and pathogenesis of prion diseases, Am. J. Pathol. 146 (1995) 785–811.
[62] J.L. Jimenez, G. Tennent, M. Pepys, H.R. Saibil, Structural diversity of ex vivo amyloid fibrils studied by cryo-electron microscopy, J. Mol. Biol. 311 (2001) 241–247.
[63] R.A. Bessen, G.J. Raymond, B. Caughey, In situ formation of protease-resistant prion protein in transmissible spongiform encephalopathy-infected brain slices, J. Biol. Chem. 272 (1997) 15227–15231.
[64] J.W. Ironside, J.E. Bell, Pathology of prion diseases, in: J. Collinge, M.S. Palmer (Eds.), Prion Diseases, Oxford University Press, Oxford, 1997, pp. 57–88.
[65] E.J. Nettleton, P. Tito, M. Sunde, M. Bouchard, C.M. Dobson, M.C.V. Robinson, Characterization of the oligomeric states of insulin in self-assembly and amyloid fibril formation by mass spectrometry, Biophys. J. 79 (2000) 1053–1065.
[66] M. Zhu, P.O. Souillac, C. Ionescu-Zanetti, S.A. Carter, A.L. Fink, Surface-catalyzed amyloid fibril formation, J. Biol. Chem. 277 (2002) 50914–50922.
[67] N. Naslavsky, R. Stein, A. Yanai, G. Friedlander, A. Taraboulos, Characterisation of detergent-insoluble complexes containing cellular prion protein and its scrapie isoform, J. Biol. Chem. 272 (1997) 6324–6331.
[68] N. Stahl, D.R. Borchelt, S.B. Prusiner, Differential release of cellular and scrapie prion protein from cellular membranes by phosphatidylinositol-specific phospholipase C, Biochemistry 29 (1990) 5405–5412.

[69] J. Safar, M. Ceroni, D.C. Gajdusek, C.J. Gibbs, Differences in the membrane interaction of scrapie amyloid precursor proteins in normal and scrapie- or Creutzfeldt–Jakob disease-infected brains, J. Inf. Dis. 163 (1991) 488–494.
[70] B. Caughey, Cellular metabolism of normal and scrapie-associated forms of PrP, Sem. Virol. 2 (1991) 189–196.
[71] S.L. Shyng, M.T. Huber, D.A. Harris, A prion protein cycles between the cell surface and an endocytic compartment in cultured neuroblastoma cells, J. Biol. Chem. 268 (1993) 15922–15928.
[72] J. Kazlauskaite, T.J.T. Pinheiro, Aggregation and fibrillization of prion proteins in lipid membranes, Biochem. Soc. Symp. 72 (2004) 211–222.
[73] P. Critchley, J. Kazlauskaite, R. Eason, T.J.T. Pinheiro, Binding of prion proteins to lipid membranes, Biochem. Biophys. Res. Commun. 313 (2004) 559–567.
[74] C. Sunyach, A. Jen, J. Deng, K.T. Fitzgerald, Y. Frobert, J. Grassi, M.W. McCaffrey, R. Morris, The mechanism of internalization of glycosylphosphatidylinositol-anchored prion protein, EMBO J. 22 (2003) 3591–3601.
[75] E. Paramithiotis et al., A prion protein epitope selective for the pathologically misfolded conformation, Nat. Med. 9 (2003) 893–899.
[76] J.I. Guijarro, M. Sunde, J.A. Jones, I.D. Campbell, C.M. Dobson, Amyloid fibril formation by an SH3 domain, Proc. Natl. Acad. Sci. USA 95 (1998) 4224–4228.
[77] M. Fandrich, C.M. Dobson, The behaviour of polyamino acids reveals an inverse side chain effect in amyloid structure formation, EMBO J. 21 (2002) 5682–5690.
[78] B. Caughey, P.T. Lansbury Jr., Protofibrils, pores, fibrils and neurodegeneration: separating the responsible protein aggregates from the innocent bystanders, Annu. Rev. Neurosci. 26 (2003) 267–298.
[79] M. Stefani, C.M. Dobson, Protein aggregation and aggregate toxicity: new insights into protein folding, misfolding diseases and biological evolution, J. Mol. Med. 8 (2003) 678–699.
[80] S.A. Priola, B. Chesebro, B. Caughey, A view from the top–prion diseases from 10,000 feet, Science 300 (2003) 917–919.
[81] A. Aguzzi, M. Heikenwalder, Cannibals and garbage piles, Nature 423 (2003) 127–128.
[82] A. Aguzzi, C. Weissmann, Prion research: the next frontiers, Nature 389 (1997) 795–798.
[83] G. Legname, I.V. Baskakov, H.O.B. Nguyen, D. Riesner, F.E. Cohen, S.J. DeArmond, S.B. Prusiner, Synthetic mammalian prions, Science 305 (2004) 673–676.
[84] J. Couzin, An end to the prion debate? Don't count on it, Science 305 (2004) 589.